CHAPTER 2
NUMERICAL MODEL OF GEOTECHNICAL CONDITIONS AND STRESS BEFORE MINING

2.1 SUMMARY

In this chapter, the virgin stress state in a rockmass containing undulated strata is analysed using the finite difference method, FLAC^{2D} (Itasca, 1999). The modelled strata undulations have limb dip angles of 5^0 and 15^0, while a literature survey reveals that a horizontal to vertical stress ratio of 2 will be reasonable to assume for the model. The chapter presents examples of the stress state on a horizontal profile line 30m deep for the unmined state. The model applies the “ubiquitous joints” model in FLAC to model the shale layer overlying the top and middle coal seams so that the plane of weakness lies parallel to sedimentation. The results show a concentration of the vertical component and a decrease in horizontal stress component at the undulated formation crest before mining. In the virgin state, shear stress is developed along the limbs of the undulated strata as a result of undulation.

2.2 INTRODUCTION

Analysis of geotechnical problems with the use of the Finite Difference method has been widely accepted in the research field for many years. Unfortunately, its regular use in geotechnical practice for stress analysis and its influence on predicting slope stability still remains limited. The reason for this lack of application is not entirely clear; however, practicing engineers are often sceptical of the need for such complexity, especially in view of the poor quality of soil and rock property data often available from routine site investigations. Although this scepticism is often warranted, there are certain types of geotechnical problems for which the finite difference approach offers real benefits. The challenge for an experienced engineer is to know which kind of problem would benefit from finite difference treatment and which would not. As a guide, Stead et al. (2001) presented a detailed review of all calculating techniques and the particular application of these techniques to slope stability analyses.

In general, linear problems such as the prediction of settlements and deformations (Barla and Chiriotti, 1995), the calculation on flow quantities due to steady seepage (Andrade et al., 2000), or the study of transient effects due to consolidation (Carranza-Torres et al. 1997) are highly favourable to solution by the finite difference method. Traditional approaches involving charts, tables, or graphical methods will often be adequate for routine problems, but the finite difference approach may be valuable if difficult geometries or material variations are encountered. Such

cases are not normally covered by traditional solutions, which is the case with a state of stress in a slope profile with an embedded weak layer and defined anisotropy near an inclined surface.

2.3 MODEL DEVELOPED FOR VIRGIN STRESS ESTIMATION

The rock properties used in this development are defined by six parameters, and shown in Table 2.1. Following shear test results (Karparov, 1998), it was estimated that the shale specimens would have approximately 30% lower shear strength parallel to bedding, compared to the shear strength normal to bedding. For simulating this anisotropy, the application of the "ubiquitous joints" model in FLAC (Itasca, 1999) has been used with the properties set out in Table 2.2. In this model, which accounts for the presence of an orientation of weakness in a FLAC Mohr-Coulomb model, yield may occur in either the solid or along the weak plane, or both, depending on the stress state.

Table 2.1 Geotechnical properties of rock in slope

	Shale	**Sandstone**
Bulk modulus – Pa	4.5E+09	5.9E+09
Shear modulus – Pa	2.3E+09	5.2E+09
Tensile strength - Pa	3.5E+06	5.5E+06
Cohesion – Pa	0.44E+06	0.70E+06
Friction angle - deg.	14	22
Density - kg/m^3	2700	2600

The use of this model was very important to the stress analysis and the type of failure in a slope profile. For this reason, the model was firstly investigated by comparing calculated results from FLAC simulating the uniaxial compressive test with a theoretical development in Jaeger and Cook (1979), in order to confirm the validity of the model with the “ubiquitous joints” option.

The uniaxial compressive strength of a shale sample with a defined plane of weakness is a function of the angle formed by the major principal stress and the plane of weakness. In FLAC, this behaviour was modelled by considering the sample as a continuum with a plastic anisotropy in the direction of the weakness. The rock sample has a height to width ratio of 2 (five zones in horizontal and ten zones in vertical direction) with the weak plane properties given in Table 2.2 below.

Table 2.2 Ubiquitous joint properties

Tensile strength (σ_{tj})	1.0 MPa
Cohesion (c_j)	0.1 MPa
Friction angle (ϕ_j)	9^0
Dilation angle (φ_j)	0^0

It is difficult, if not impossible, to correlate the results of different types of direct and indirect tensile tests on rock using the average tensile strength as the basic material property. Hardy (1973) was able to obtain good correlation between the results of a range of tests involving tensile fracture when the apparent surface energy was used, based on the Griffith (1924) theory for fracture propagation, as the unifying material property. The Griffith theory predicts that

the uniaxial compressive stress at the crack extension will always be eight times the uniaxial tensile strength. This does not agree with laboratory results, which have given the widely accepted tensile strength as one-tenth the uniaxial compressive strength. The tensile strength used in the FLAC model is therefore assumed to be one-tenth the uniaxial compressive strength.

The calculations are performed under plane strain conditions where the plane-of-weakness model (Jaeger and Cook, 1979) predicts that slip will occur in a triaxial test, provided that $\left(1-\tan\phi_j \tan\beta\right)>0$ and:

$$\sigma_1 = \sigma_3 - \frac{2\left(c_j + |\sigma_3| \tan\phi_j\right)}{\left(1-\tan\phi_j \tan\beta\right)\sin 2\beta} \qquad (2.1)$$

where β is the angle formed by the direction of σ_1 and the joint.

For those combinations of c_j, ϕ_j, σ_3 and β for which Equation 2.1 is not satisfied, slip in the joint cannot occur, and the only alternative is the failure of the rock material which, according to the Mohr-Coulomb failure criterion, will occur for

$$\sigma_1 = \frac{1+\sin\phi}{1-\sin\phi}\sigma_3 - 2c\sqrt{\frac{1+\sin\phi}{1-\sin\phi}} \qquad (2.2)$$

where c is intact material cohesion, and ϕ is the intact material angle of internal friction.

In the uniaxial compression test, σ_3=0, so Equations 2.1 and 2.2 can be rewritten as:

$$\sigma_1 = \frac{-2c}{\left(1-\tan\phi_j \tan\beta\right)\sin 2\beta} \tag{2.3}$$

and

$$\sigma_1 = -2c\sqrt{\frac{1+\sin\phi}{1-\sin\phi}} \tag{2.4}$$

The maximum pressure for a uniaxial compressive test (σ_c) of a rock sample with a weak plane will then be:

$$\sigma_c = \begin{cases} \min\left[2c\sqrt{\frac{1+\sin\phi}{1-\sin\phi}},\ \frac{2c_j}{\left(1-\tan\phi_j \tan\beta\right)\sin 2\beta}\right] & \text{if } \left(1-\tan\phi_j \tan\beta\right)>0 \\ 2c\sqrt{\frac{1+\sin\phi}{1-\sin\phi}} & \text{if } \left(1-\tan\phi_j \tan\beta\right)<0 \end{cases} \tag{2.5}$$

The FLAC model is loaded with constant velocity boundaries at the top and bottom of the model until failure occurs, and then the failure stress and type of failure mode are noted. Combined damping is used because velocity vectors are all non-zero in the final state (Itasca, 1999).

The grid is the same for all the values of β, because the material property joint angle, “jangle”, controls the inclination of the joints in this model. Fairly accurate results are obtained with only 50 elements.

The effect of the variation of β is calculated every 5^0 from 0^0 to 90^0. For this test, the failure state is reached within 4000 calculation steps for the applied

velocity loading condition. This occurs for either failure along the weak plane or within the intact material. The *FLAC* solution at each value of β is then determined at the end of each 4000-step increment.

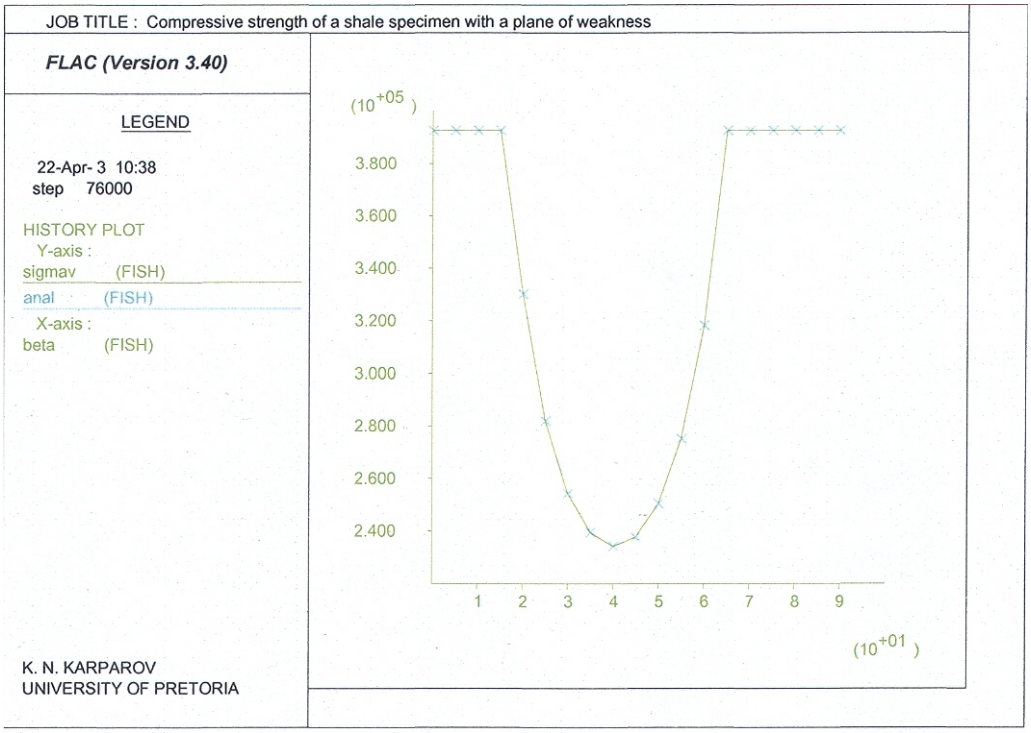

Figure 2.1

Comparison of uniaxial compressive strength values- "ubiquitous" joints model (cross) versus analytical solution (line)

A comparison of FLAC's "ubiquitous" joint model (Figure 2.1) with the analytical solution shows excellent agreement with the error below 1% for all values of β. This confirms the applicability of using the ubiquitous joints for the slope stability modelling. The input file for the vertical stress comparison between the FLAC "ubiquitous" joints model and the theoretical development in Jaeger and Cook (1979) can be seen in A1.1 (Appendix 1). It is concluded that the "Ubiquitous Joint" model in FLAC will adequately model the shale layers present in the geological succession.

2.4 ESTIMATION OF HORIZONTAL TO VERTICAL STRESS RATIO

Skempton (1961) states that Samsioe first put the idea forward in the 1930's that the k-ratio (k), defined as the ratio between the horizontal and vertical stresses in soil or rock, could be larger than unity. By reconstructing the geological history of London clay in Bardwell, Skempton (1961) showed that in this case, k > 2.5 and that the 10-15m thick upper layer of the subsoil is at the passive limit state of stress (cf. Terzaghi, 1961). Lambe and Whitman (1979) concede that in overconsolidation, the k – ratio can reach as high a value as 3.

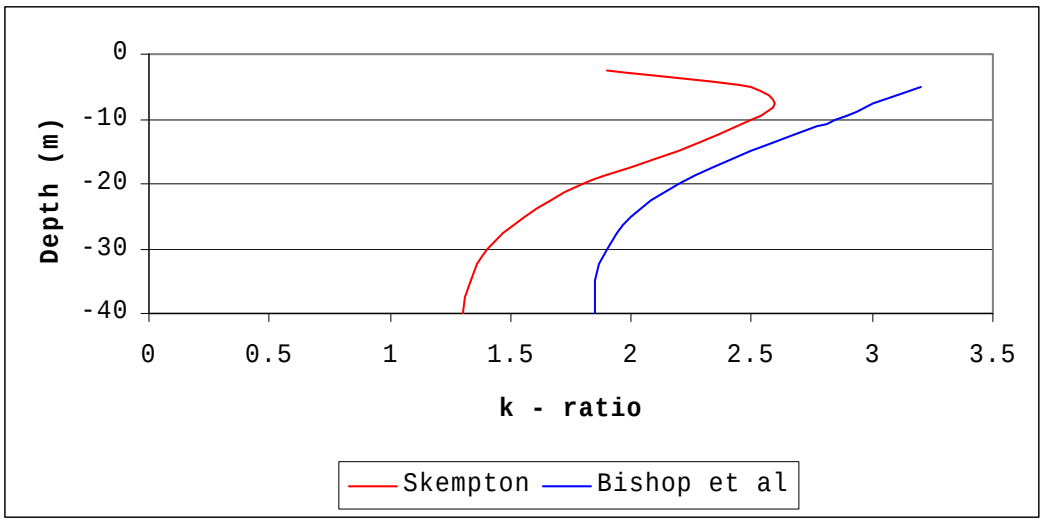

Figure 2.2
Variation of the k - ratio with depth in overconsolidated London clay, measured in a laboratory using undisturbed samples (Skempton, 1961; and Bishop et al., 1965)

The results of Skempton (1961) and Bishop et al. (1965) are reproduced in Figure 2.2, where it can be seen that the higher k–ratio value (k > 2) is observed at a depth

of 10-15m, while at a depth of 30-40m it has a value of between 1.5 and 2.0.

Brooker and Ireland (1965) claim that the magnitude of *k* is not only a function of the overconsolidation ratio but also a function of the value of the angle of internal friction as well. For an overconsolidation ratio > 8, the effect of the angle of internal friction is not certain. According to Ladd (1964), *k* becomes greater than unity for overconsolidation ratios > 2.5 - 4.5.

Broms (1971) ranged in situ k-ratios between 0.9 and 1.5, and in the laboratory between 0.45 and 2.0 by compacting loose soils behind a supporting wall. A similar effect was also observed during pile driving, even for piles of constant diameter along their whole length. Bassett (1970) estimated that *k* increases from 1 to 3.5 in the course of the process.

By applying the finite element method, Malina (1969) succeeded in numerically determining the effect of overconsolidation on the magnitude of *k*. He reports that in the vicinity of the surface, the state of stress is close to passive; this finding is in agreement with an analysis published by Skempton (1961).

In the only reference relevant to the coal mine in question, van der Merwe (2002a) mentions the applicability of a k–ratio of 2 in South African coal mines, and discusses the issue of roof stability in underground coal extraction (van der Merwe, 2002b). Because of the varied *k*-ratio estimates above, the fact

that nearly all data refers to clays in civil engineering scenarios, and that there is virtually no k-ratio data for surface mines excepting van der Merwe's (2002a) results, the author has decided to apply a k-ratio of 2 in all models in this thesis. This decision is reviewed in Chapter 3, where the effects of the presence of a mined slope are modelled.

2.5 GRID DEVELOPMENT FOR A MODEL WITH UNDULATED STRATA

In order to undertake objective analyses of virgin stress before mining, it is necessary to develop a model that contains the essential features of the geological structure. Requirements for a reasonable model of the undulating strata in the mine are as follows:

- The layers should dip smoothly without any sharp kinks causing stress concentrations.
- The strata should become flatter with decreasing depth, eventually becoming horizontal on the surface (this is a feature of the sedimentation overlying the undulating dolomitic palaeo-surface described in Chapter 1).
- The layers should be thinner in the crests of the undulated strata formation, and thicker in the troughs, as was observed at the colliery.

These three grid conditions should be constructed in the centre of the model to avoid the influence of boundary conditions, and at the same time, to allow space for the slope face (highwall) to approach the undulated surface. A FISH function (Itasca, 1999) with

boundaries as shown in Figure 2.3 was written to fulfil the above-mentioned three requirements for the case of 15^0 limb inclination of the undulated strata formation. The FLAC input file with FISH function can be seen in Appendix 1, Section A1.1.2.

Figure 2.3
Boundary of FLAC model with angulated surface, creating 15^0 strata inclination at 30m depth along profile line A-A, and flat to near-flat strata at surface

The function's major advantage is its capability to place this formation at any point on the bottom boundary of the model and control its altitude to achieve the required inclination at a chosen depth. At the bottom boundary the inclination of the rows of finite difference zones are much steeper, but their inclination gradually decreases closer to the ground surface, where they are horizontal. The required dip angle of the rows (representing sedimentary layers) in the grid is achieved at a depth of 30m. Finally, the rows above the crest are thinner, compared to the rows above the "troughs", which are here modelled by the ends of the FISH-generated domical structure.

2.6 VIRGIN STRESS DISTRIBUTION IN MODEL

To verify the reliability of the new grid for its further application, a model with homogeneous material was run first. The undulated strata formation was chosen to have maximum limb inclination angles of 5^0 and 15^0 at the intersection with the horizontal line A-A at a depth of 30m (See Figure 2.3). The finite difference grid consists of 25000 1m x 1m zones, which correspond to 250m in length and 100m in height respectively, with the undulated strata formation positioned between 130m and 230m from the left model boundary. The trial run of these examples used geotechnical parameters for massive sandstone (Table 2.1), a k-ratio of 2 and an unmined ground surface. Such a long model has been chosen to accommodate the undulated strata and for modelling an advancing excavation cut approaching this formation.

To evaluate the magnitude of stress variations induced by the geological conditions, a stress concentration coefficient for vertical and horizontal stress components was used, which has the form of:

$$k_{\mathrm{V}}^{*} = \frac{\sigma_{\mathrm{V}}^{\mathrm{F}}}{\sigma_{\mathrm{V}}} \quad \text{or} \quad k_{H}^{*} = \frac{\sigma_{H}^{F}}{\sigma_{H}} \tag{2.6}$$

where k_V^* and k_H^* are stress concentration coefficients for vertical and horizontal stress components respectively; σ_V^F and σ_H^F are vertical and horizontal stress components calculated by FLAC; and σ_V and σ_H are the virgin vertical and horizontal stresses. According to Ugular (1999), this coefficient can be applied as long as the shape variation is gradual,

which is satisfied by the undulated formation created with the FISH function. Changes in layer thicknesses together with a dip angle on the top and bottom contact surfaces between the shale and middle coal seam are set out in Table 2.3.

The virgin stress components calculated in the FLAC model were compared with expected results using the relationships $\sigma_V = \rho g h$ and $\sigma_H = 2\sigma_V$, with good agreement obtained away from the undulating strata formation.

Figure 2.4 shows the basic characteristics of the stress distributions along the profile line A-A shown in Figure 2.3, assuming an undulating homogeneous sandstone formation. Figure 2.4a gives an example of vertical stresses at 30m depth for 5^0 and 15^0 limb inclinations. The figure shows that there is a high stress region at the formation's crest. At the trough of the undulated strata a decrease in vertical stress is present. From the figure it can be seen that the stress concentrations are a function of the strata inclination angle. All the vertical stress plots for different model geometries are shown in Appendix 2, Figures A2.1 and A2.2.

Table 2.3 Seam thickness and layer inclination variations taken from the trough to the crest of the undulated strata model

Distance from the trough (m)	UGS with 5^0 limb inclination					UGS with 15^0 limb inclination				
	Thickness at the trough 2m	Thickness at the trough 8m	Dip of strata on contact (deg)			Thickness at the trough 2m	Thickness at the trough 8m	Dip of strata on contact (deg)		
			Bottom	Top 2m thick	Top 8m thick			Bottom	Top 2m thick	Top 8m thick
0	2.00	8.00	5.15	5.15	4.01	2.00	8.00	15.65	14.58	11.87
2	1.98	7.95	5.15	5.15	4.01	1.96	7.85	15.65	14.58	11.87
4	1.98	7.90	5.71	4.58	4.01	1.92	7.70	15.65	14.58	11.32
6	1.96	7.85	5.15	4.58	3.44	1.89	7.55	15.12	14.04	11.32
8	1.95	7.80	5.15	4.58	4.01	1.85	7.41	15.12	14.04	11.32
10	1.94	7.76	5.15	4.58	3.44	1.82	7.27	14.58	13.50	10.76
12	1.93	7.72	5.15	4.58	3.44	1.79	7.14	14.58	12.96	10.21
14	1.92	7.67	4.58	4.01	3.44	1.75	7.00	13.50	12.96	10.21
16	1.91	7.62	4.58	4.01	3.44	1.72	6.87	12.96	11.87	9.65
18	1.90	7.58	4.01	3.44	3.44	1.69	6.75	12.41	11.32	9.09
20	1.89	7.55	4.01	3.44	2.86	1.66	6.64	11.87	10.76	8.54
22	1.88	7.51	3.44	3.44	2.86	1.63	6.53	10.76	10.21	7.97
24	1.86	7.47	3.44	3.44	2.86	1.60	6.42	10.21	9.65	7.97
26	1.86	7.45	3.44	2.86	2.29	1.58	6.33	9.09	8.54	6.85
28	1.85	7.42	2.86	2.86	1.72	1.56	6.25	8.54	7.97	6.28
30	1.84	7.39	2.29	2.86	1.72	1.54	6.17	7.41	7.41	5.71
32	1.85	7.37	2.29	1.72	1.72	1.53	6.10	6.85	6.28	5.15
34	1.84	7.35	1.72	1.72	1.15	1.51	6.04	5.71	5.15	4.01
36	1.83	7.32	1.15	1.15	1.72	1.49	5.98	4.58	4.58	4.01
38	1.83	7.31	1.15	1.15	1.15	1.49	5.94	4.01	3.44	3.44
40	1.83	7.31	1.15	1.15	0.57	1.48	5.91	3.44	2.86	2.29
42	1.82	7.29	0.57	0.57	0.57	1.47	5.88	2.29	1.72	1.72
44	1.82	7.29	0.57	0.57	0.57	1.46	5.86	1.15	1.15	1.15
46	1.82	7.28	0.00	0.00	0.00	1.46	5.85	0.00	0.00	0.00
48	1.82	7.28	0.00	0.00	0.00	1.47	5.85	0.00	0.00	0.00

a)

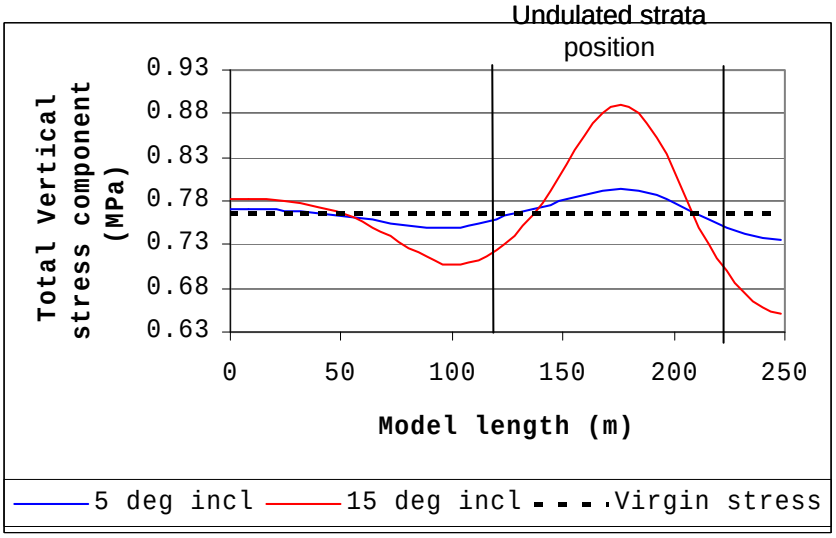

b)

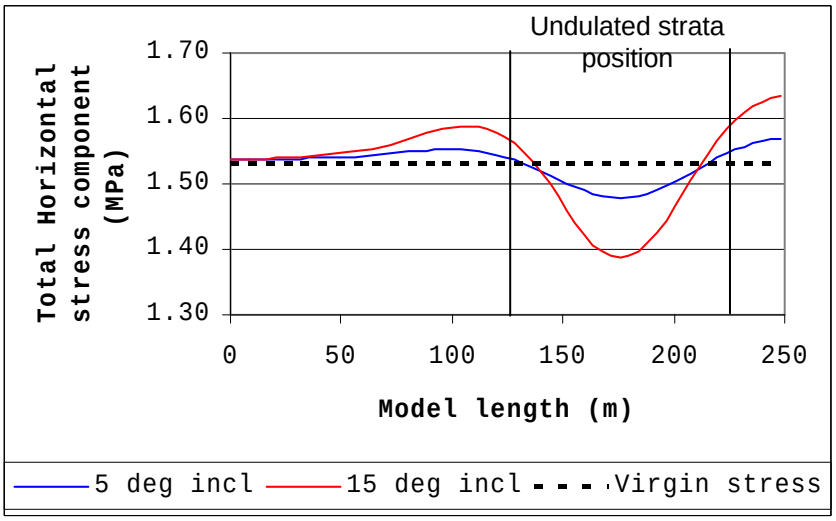

c)

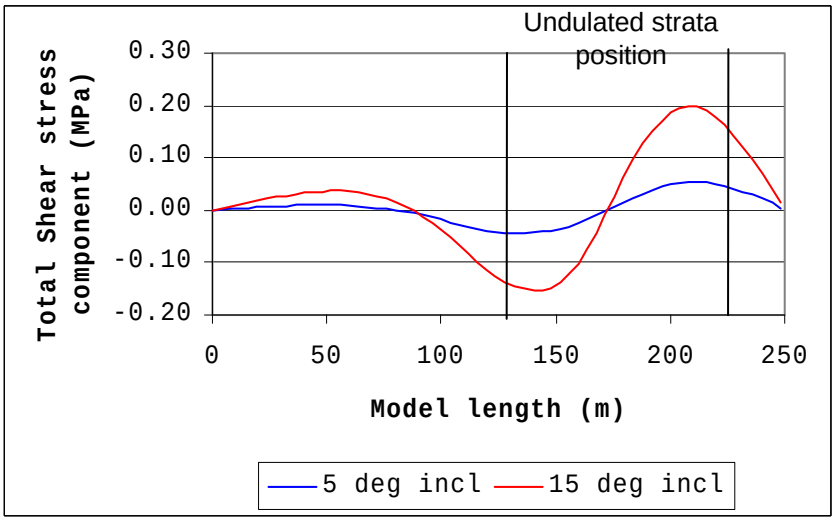

Figure 2.4

Stress state along horizontal line at 30m depth

Such an increase in vertical stresses was calculated by Timoshenko (1934) using the theory of elasticity for pressure between two spherical bodies in contact, as a sphere with smaller diameter is in contact with and enclosed by sphere with larger diameter. Depending on the radius of spheres (in our case, changes in a layer's thickness) and their elastic constants, the vertical stress can increase up to 25% for a depth of 30m. Elastic properties were taken from Table 2.1 and the applied compressive force was equal to 765180N, corresponding to a depth of 30m. The calculated results can be seen in Table 2.4, where the percentage difference between Timoshenko's model and the stresses calculated by FLAC is less than 5%.

Table 2.4 Comparison of the stress calculated by FLAC and the re-worked Timoshenko's model

UGS* incl. (..^{0})	Radius R_1 (m)	Radius R_2 (m)	Stress after Timosh-enko	Calc. str. by FLC	Differ (%)
5	431.4	439.9	0.811 Mpa	0.793 MPa	-2.1
15	122.1	122.8	0.869 Mpa	0.896 MPa	3.2

* Undulated ground surface

Figure 2.4b shows the horizontal stress component. The low-stress region can be seen at the formation crest while the high-stress region can be seen at the formation lows.

Figure 2.4c shows the shear stress results. Pre-existing shear stress in virgin stress conditions on the limbs of the undulated formation have values of approximately 0.05MPa and 0.15MPa for layers inclined at 5^0 and 15^0 respectively. The non-zero shear stresses

develop purely as a result of the presence of the inclined layers in the geological succession, and are not tectonic in origin.

For the pre-existing shear stress verification along the limbs of the undulated strata, a shale core from the mine was cut parallel to bedding, glued on thin glass, and polished to form a thin section. Under the binocular microscope and normal lighting (Picture 2.1), the original grain direction is visible and marked with the red line S0. “CS” zones (marked with green) indicate post-sedimentation shear stress development. Using the rotating polariser as a tool for structural analysis permits the simultaneous examination of features such as grain size, grain shape, grain identity and the *c*–axis (Fueten and Goodchild, 2001).

The newly developed carbon crystals (Picture 2.2) with a direction of approximately 45^0 to the direction of the sedimentation (shown by the dotted yellow lines marked S1) are the result of the existence of the post-sedimentation shear, which also confirms the shear stress along the limb of the undulated stratum in virgin conditions.

The stress concentration coefficients for vertical and horizontal stress components, calculated from Equation 2.6 (p. 37), are presented in Figure 2.5. The figure shows that the horizontal stress component decreases in magnitude by 4% at the crest of the undulated strata formation at a 5^0 inclination, and by 10% at a 15^0 inclination, while the vertical stress component increases by 4% and 16% respectively for the same limb inclinations.

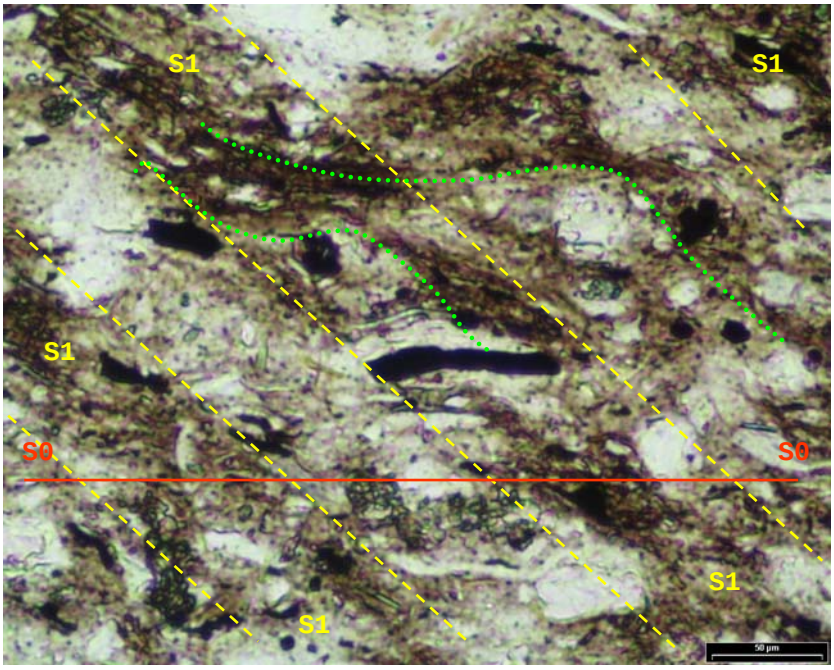

Picture 2.1

Microscopic picture of a shale specimen from undulated stratum showing shear bands and carbon flakes orientated parallel to sedimentation direction S0

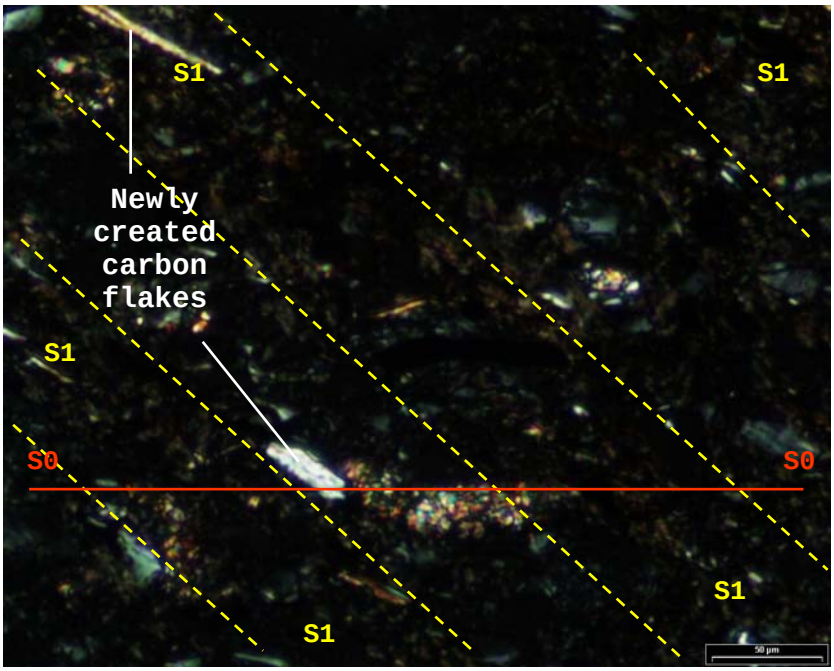

Picture 2.2

Carbon flakes at 45° to bedding direction S0

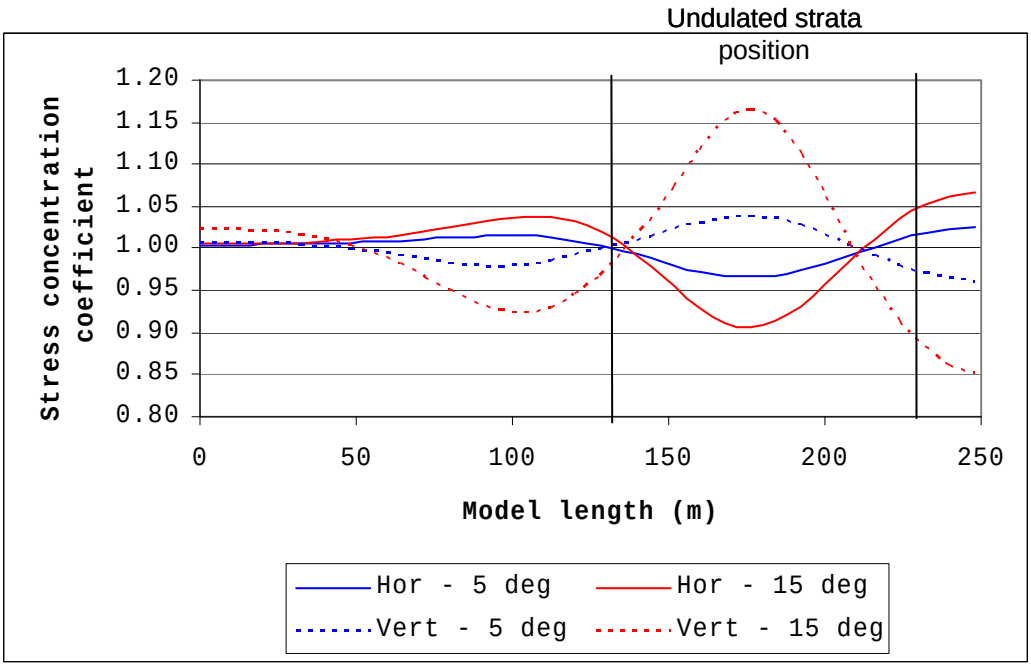

Figure 2.5

Horizontal and vertical stress concentration coefficients along horizontal line at 30m depth

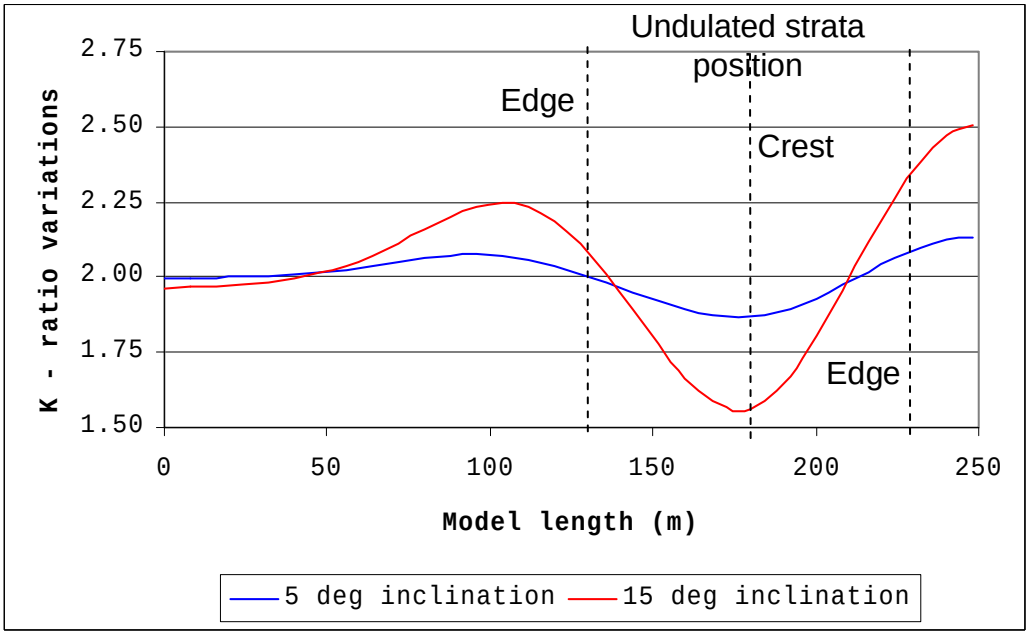

Figure 2.6

K-ratio variations along horizontal line at 30m depth

Because of the vertical stress increases and horizontal stress decreases, the k-ratio drops to a value of 1.6 at the crest because of the increased vertical and reduced horizontal stresses. In the troughs of such formations, the opposite is observed; an increase in horizontal stresses and a decrease in vertical stresses can be observed, which consequently increases the k-ratio by about 10% (Figure 2.6).

In summary, there is an increase in vertical stress components and a decrease in horizontal stress components above the crest of the undulated formation. Vertical stresses are more sensitive to the changes in the dip angle of an undulated strata limb than horizontal stresses. Shear stress can be expected to develop along the formation limbs and to reach zero at the crest. This fact raises two questions about the reliability of the well-known equilibrium methods for slope stability analysis: the first, about the weight of the slices across such strata; and the second about the magnitude and distribution of interslice forces (for instance sinusoidal or trapezoidal) and their directions.

The effect of the undulating strata on the inclination of the principal stress direction and the principal stress magnitude appear in Figures 2.7 and 2.8 respectively. The principal stress angle varies as a result of the limb inclination, as the steeper undulated strata formation creates higher angle variations compared to the flatter formation (Figure 2.7). It is seen that both graphs have “zero” value at the formation crest, which confirms the higher value of the horizontal stress component compared to the

vertical stress component. Therefore, we can draw the conclusion that the principal stress directions tend to follow the bedding. This conclusion is another confirmation of the existence of shear stress along the horizontal line A-A shown in Figure 2.3. The pre-existing shear along the undulating strata limbs would not have been included in the traditional slope stability analyses, which assume the overburden weight for the vertical stress, and an assumed k-ratioto estimate the horizontal stress.

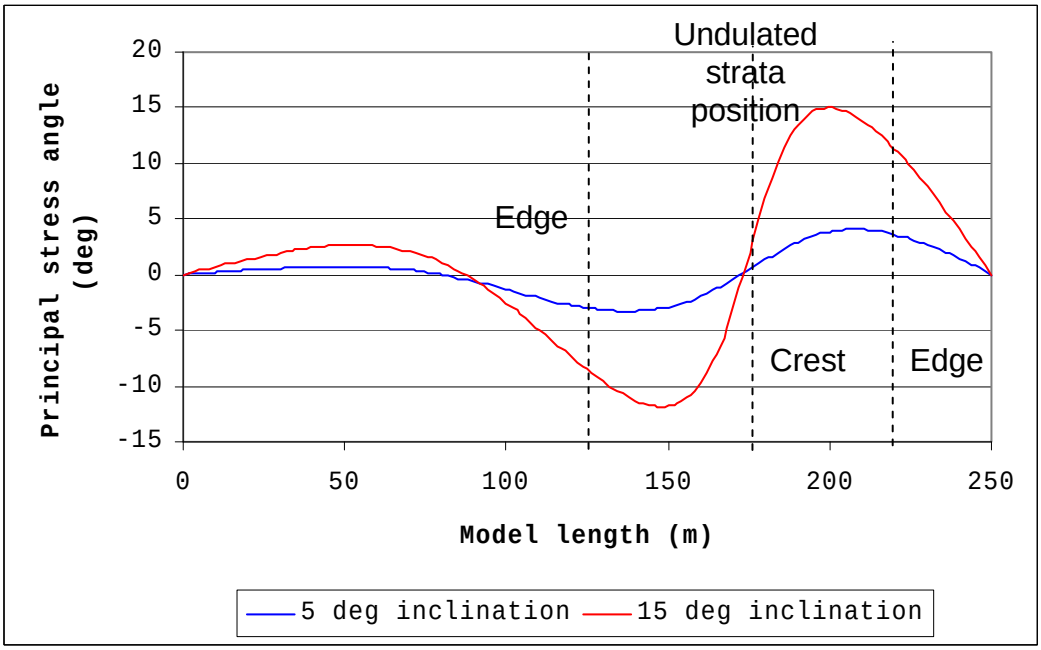

Figure 2.7

Principal stress angle variations along horizontal line at 30m depth

The magnitude of the principal stress variations (Figure 2.8) is also influenced by the formation limb inclinations. The steeper limbs create higher principal stress variations compared with the flatter limb inclinations.

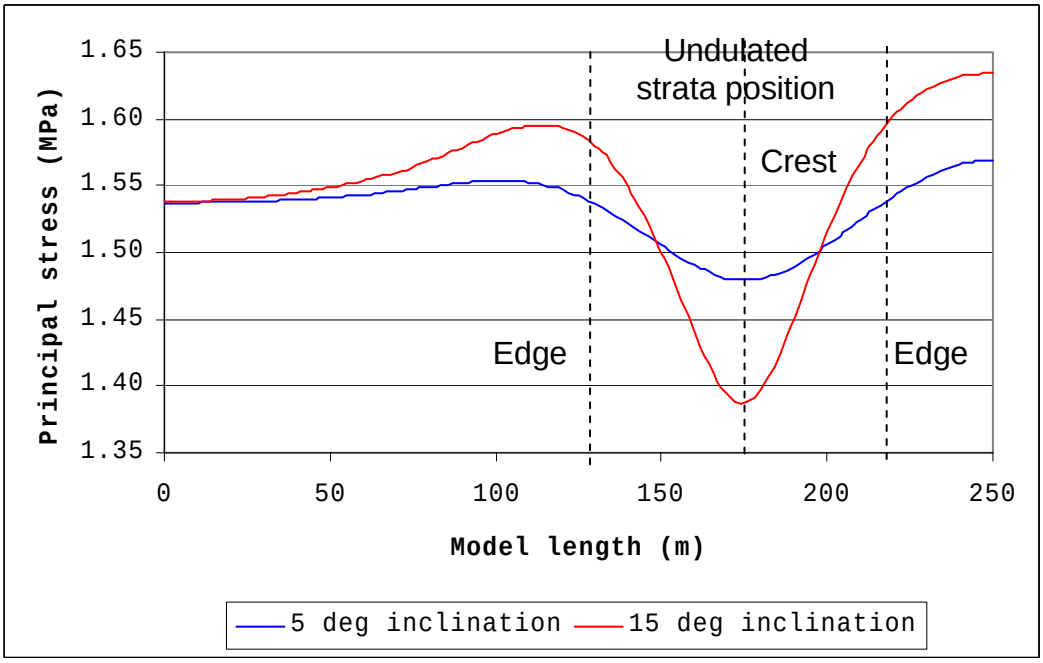

Figure 2.8
Major principal stress magnitude variations along horizontal line at 30m depth

2.7 VIRGIN STRESS ON AND ABOVE SHALE-COAL CONTACT

Failure in the mine took place on the bottom contact of the shale layer (i.e. at the top of the middle coal seam) when the strata were dipping toward the pit. This section concentrates on the virgin stress state along this contact, and along a vertical line above the crest of the undulating formation.

Figure 2.9 presents part of the model showing the shale layer, indicating the future slope position and the two profile lines for the representation of virgin and post-mining stress state data. The thickness of the embedded shale layer (h) in the first run of the model was 2m and, in the second run, 8m with an overburden thickness (H) of 28m and 22m respectively. In figure

2.9, the mine slope angle β has been given two values – 70^0 and 90^0, and the effects of slope angle will be investigated in Chapter 3. The strata inclinations on the limb, defined by α in the slope profile are 5^0 and 15^0.

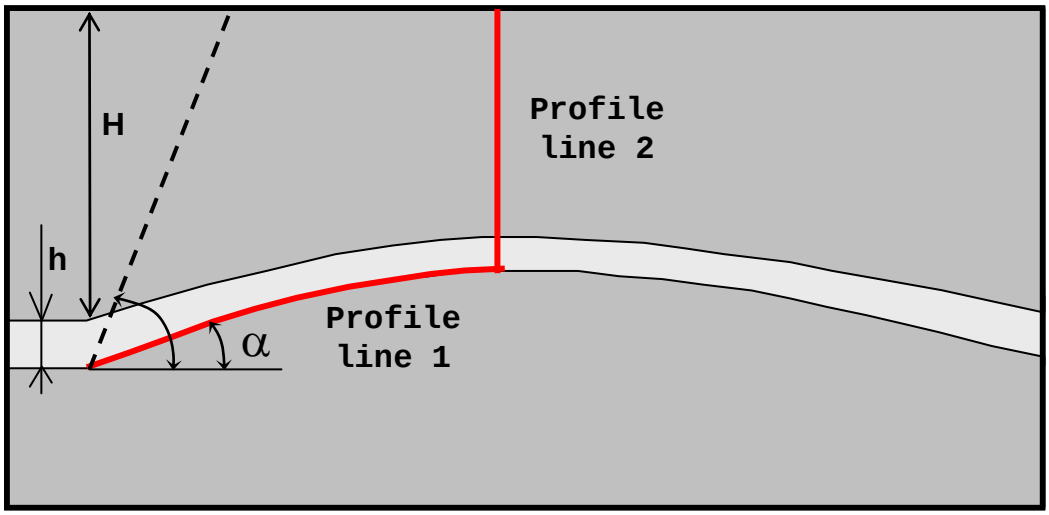

Figure 2.9
Definition of profile lines and model parameters for undulating strata

Turning to the virgin stress along profile line 1 on the contact, the plots given in Figure 2.10 indicate that the vertical stress is influenced by the presence of the undulating strata. Using equation 2.6, and expressing this stress as a dimensionless stress concentration factor produces the result shown in Figure 2.11. In the figure the formation with steeper limbs causes a higher stress concentration at the crest compared to the the formation with the flatter limbs. The shale thickness is insignificant according to the model results.

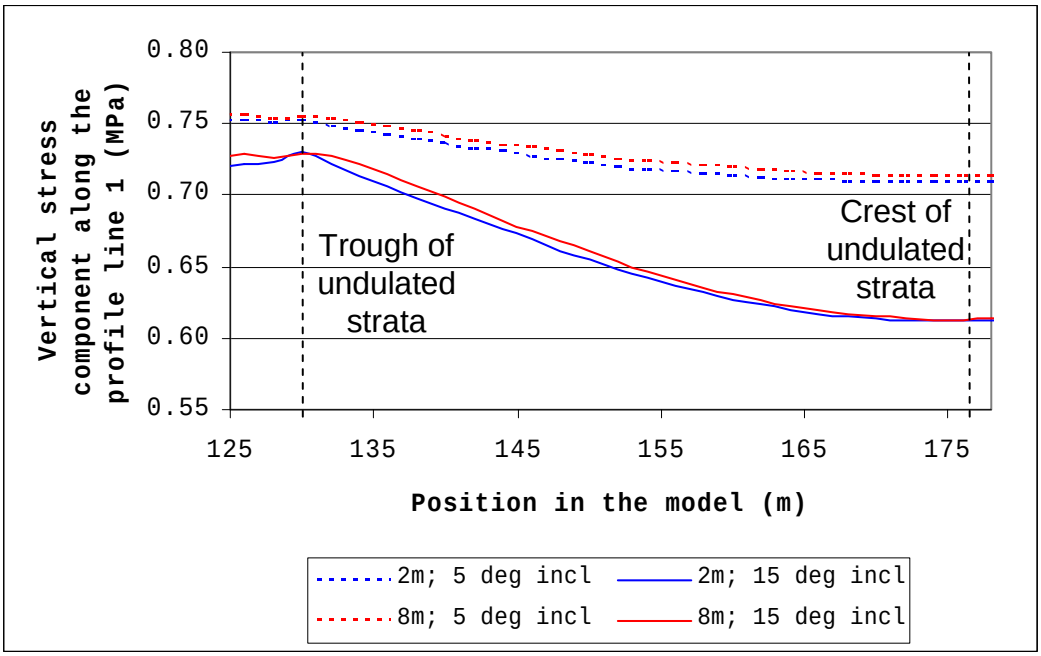

Figure 2.10

Vertical stress component before mining along a profile line set at the shale-middle coal seam contact

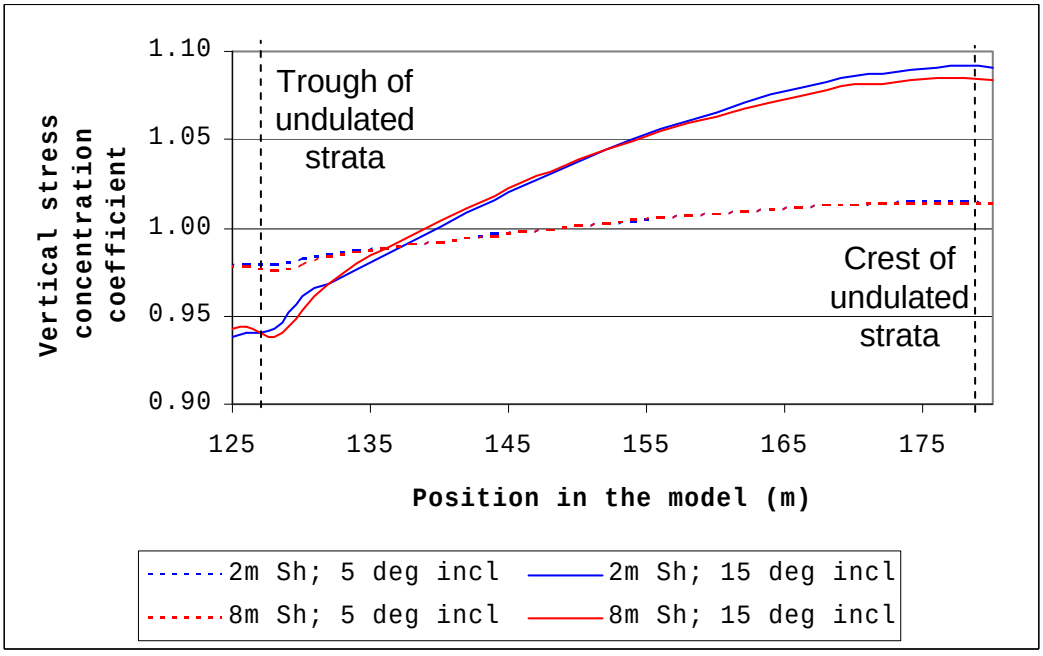

Figure 2.11

Vertical stress concentration factor before mining along a profile line on the shale-middle coal seam contact

The virgin vertical stress component distributions computed for all possible scenarios appear in Appendix 2, Figures A2.27-A2.30.

Figure 2.12 presents horizontal stress components along profile line 1 in virgin stress conditions. Along the formation limb, layers with a steeper inclination angle have lower horizontal stress in the formation crest compared to the formation with flatter inclination. This lower horizontal stress is the result of the smaller depth of the formation crest in the model with steeper limbs compared to the crest depth of the flatter formation.

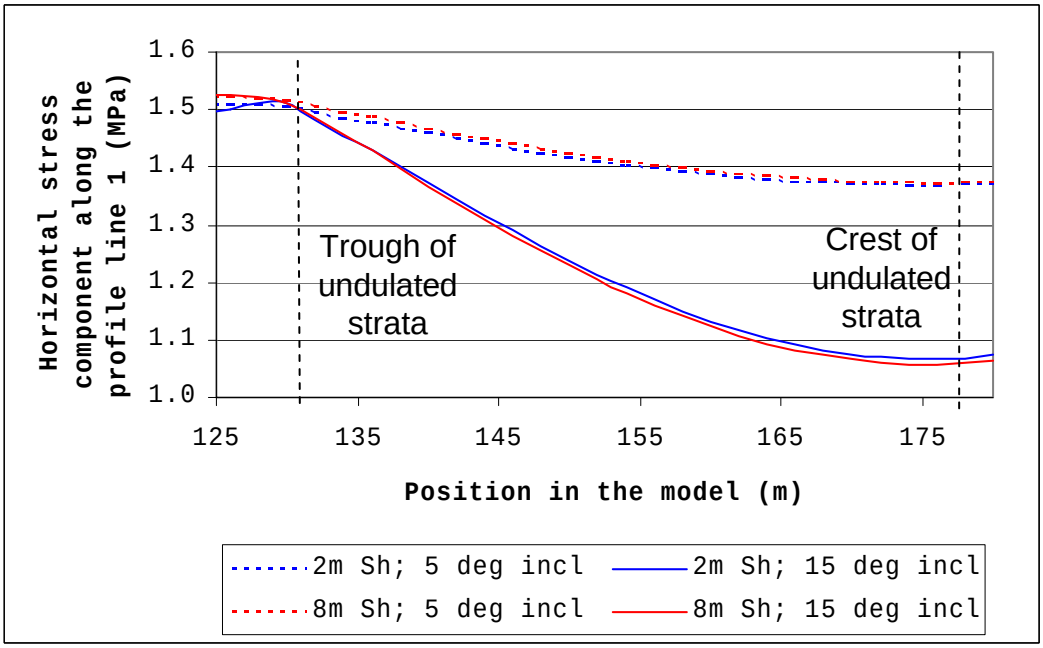

Figure 2.12
Horizontal stress component before mining along the profile line set at shale-middle coal seam contact

If we compare the layers with different thickness along the formation limb, the thicker shale layer has a lower horizontal stress component at the crest compared to the thinner layer. Equation 2.6 is used again to

investigate the undulated strata formation influence on concentrating the horizontal stress component in virgin conditions

Figure 2.13 presents the plot of these stress concentration coefficients. In the figure the horizontal stresses are reduced by 10% to 30% at the formation crest for a 2 m and 8 m thick layer respectively.

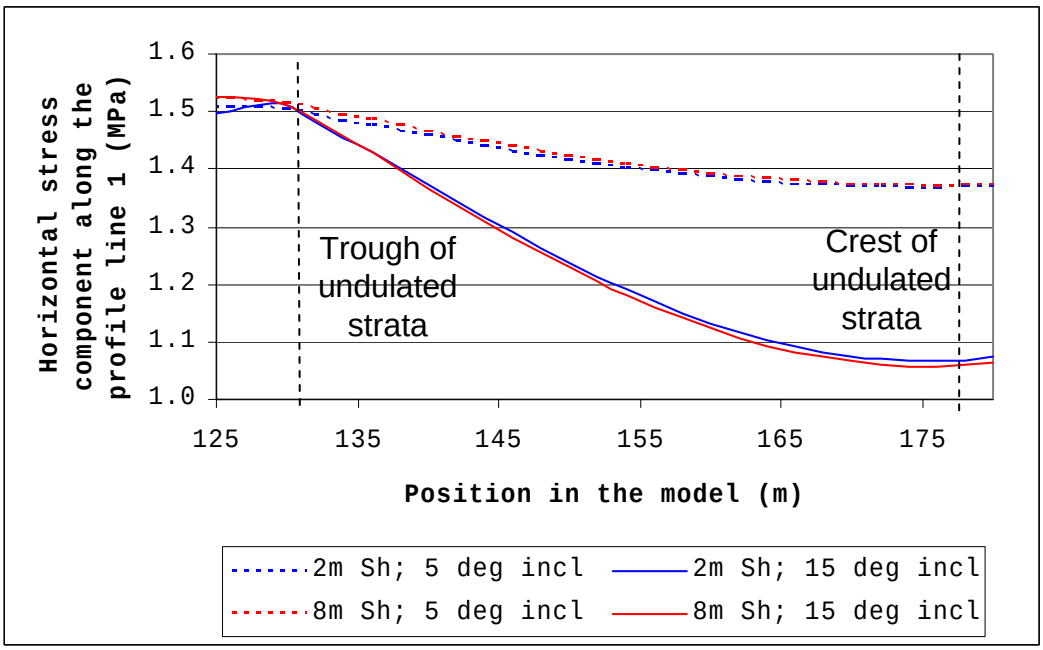

Figure 2.13
Horizontal stress concentration factor before mining along the profile line set at the shale-middle coal seam contact

The thicker embedded layer has a higher offloading effect in the crest of the undulating formation compared to the formation with the thinner embedded layer, while there is little effect on the horizontal stresses in the trough.

Therefore, we could say that the formation crest is subject to about 1% to 9% increased loading of the vertical stress component and 10% to 30% offloading of the horizontal stress component for limb angles of 5° and 15° respectively. This means that the virgin stress state is closer to lithostatic conditions for virgin stresses with a k-ratio of 2 because of the presence of the formation.

The horizontal stress component distribution in the model with a 2m and an 8m embedded shale layer and limb inclinations of 5^0 and 15^0 are detailed in Figures A2.31-A2.34, Appendix 2. Like Figure 2.13, all these figures show the presence of an induced tensile horizontal stress above the formation crest.

There is no closed-form method to calculate the shear stress component in virgin stress conditions, but it is reasonable to assume that the vertical and horizontal stress components are the principal stresses. Therefore, shear stresses must develop along the limbs of the undulating palaeosurface and in the inclined sediments overlying it.

Figure 2.14 shows plot of the shear stress component along the profile line at the base of 2m- and 8m-thick shale layers. It can be seen that the profile with the thicker embedded shale layer always has lower shear stress along the profile line compared to the profile containing the thinner layer. The highest shear stress develops at the formation toe, while the steeper limb inclination has a higher shear stress component than the to the flatter limb.

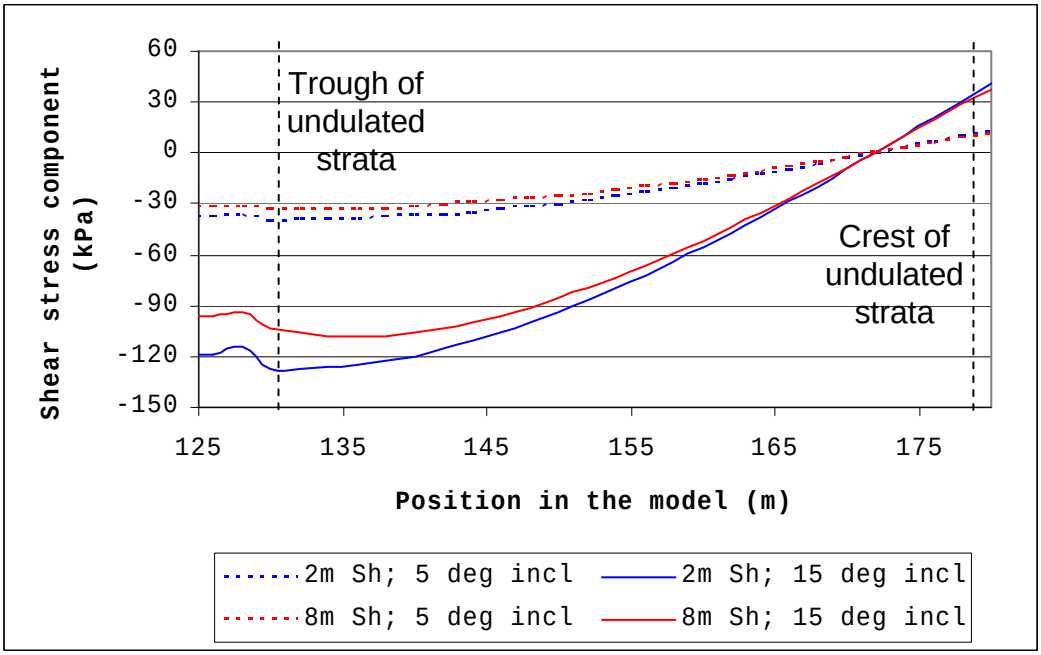

Figure 2.14

Shear stress component before mining along a profile line set at the base of the weaker layer

Theoretically, at the formation crest we should not have any shear stress, which is not confirmed by Figure 2.14 but this shear stress is very low (in the range of 10-20kPa) and can be ignored. In the formation trough there is a maximum shear stress component which is influenced by the limb inclination. The shear stress components for all possible scenarios appear in Figures A2.35-A2.38, Appendix 2.

Considering stress above the undulating formation, Figure 2.15 shows a plot of the virgin horizontal stress component along a vertical profile line (profile line 2, see Figure 2.9) above the crest of the undulating formation. The model predicts that a small tensile stress develops close to the ground surface above the formation crest in virgin conditions. The tensile zone depth is roughly proportional to the limb

inclination angle, as the steeper undulated strata formation creates a larger tensile zone at surface.

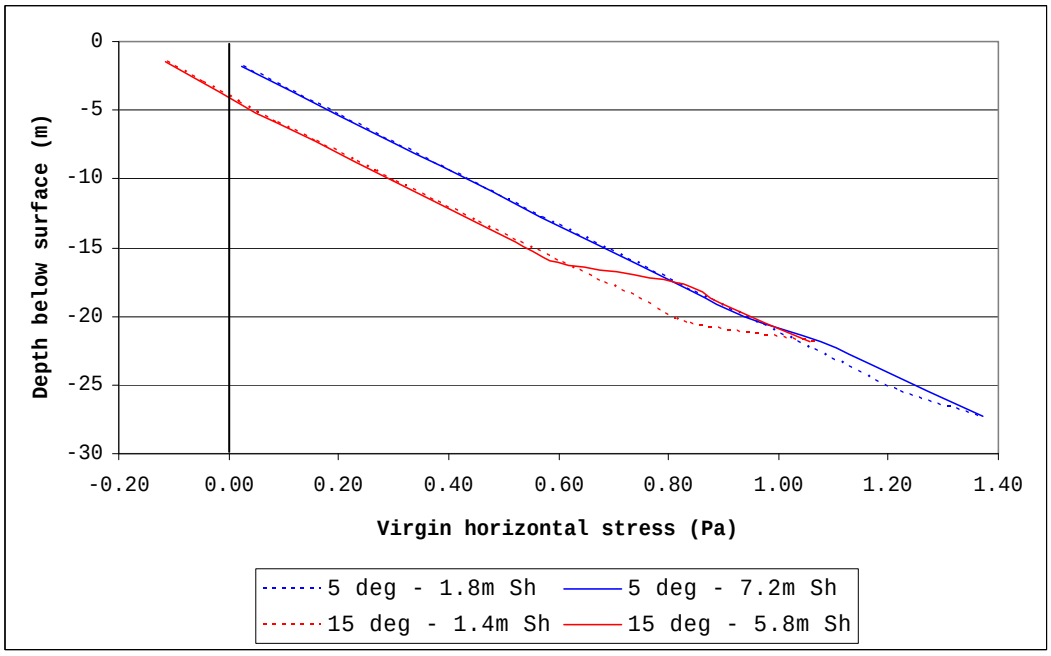

Figure 2.15

Horizontal stress component in virgin stress conditions along a vertical profile line above formation crest

In Figure 2.15, the tensile stress on the surface created by the flatter formation is shown to be in the range of 19 – 21kPa and cannot be seen because of the scale, whereas the tensile horizontal stress above the crest bounded by steeper limbs is of the order of 100kPa.

2.8 CONCLUSIONS

In conclusion the following have been noted:

- The ubiquitous joint model was tested and shown to be in agreement with the theoretical development by Jaeger and Cook (1979). Hence, it is included in the model.

- The FISH function produces an adequate model profile for the undulating formation structure at the desired depth of interest, and along the shale-middle coal seam contact.
- Stress deviations from simple models for horizontal and vertical stresses are the result of model geometry and not of tectonic stress.
- Differences in stress distribution are almost wholly the result of the geological structure, not the strata composition, i.e. whether the succession is homogeneous sandstone, or a combination of sandstone, shale, and coal.
- Stress deviations both in direction and magnitude are significant all along the limbs of the undulated strata formation, and become increasingly so with increasing limb inclination.
- The concentration of the vertical stress component at the crest is confirmed by Timoshenko (1934).
- Shear stresses develop along the limbs in virgin conditions because of the limb inclination, and this is supported by the photomicrographs in Pictures 2.1 and 2.2.
- Conditions for the development of a horizontal tensile stress on surface above the formation crest are favourable, although it is unlikely that it would exist because of weathering and sedimentation processes through geological time.
- The inability of existing slope stability methods to explain the failures observed in Chapter 1 suggests that the non-uniform virgin stress state predicted by the model must persist to some degree in the strata.

These results are all used in subsequent analyses to establish the stability of a mined slope in undulating strata.